



Cite this: *Phys. Chem. Chem. Phys.*,
2015, 17, 10426

Outside rules inside: the role of electron-active substituents in thiophene-based heterophenoquinones†

L. Colella,^{ab} L. Brambilla,^a V. Nardone,^{ac} E. Parisini,^c C. Castiglioni^a and C. Bertarelli^{*ac}

The biradicaloid vs. quinoidal character of the ground state of thiophene-based heterophenoquinones bearing donor or acceptor groups is investigated. Keeping the conjugation length fixed, namely, the 5,5'-bis(3,5-di-*tert*-butyl-4-oxo-2,5-cyclohexadiene-1-ylidene)-2,2'-dihydroxy bithiophene backbone, an opposite effect occurs depending on the donating or withdrawing nature of the substituents. The character of the ground state depends not only on the electronic nature of the substituents but also on their position on the molecular skeleton: donor groups on the 3,3'-positions of the bithiophene central core stabilize a quinoidal ground state, whereas a biradicaloid electronic structure results from the introduction of the same donor groups onto the lateral phenones. Withdrawing groups behave similar to donors, but in the opposite direction.

Received 9th December 2014,
Accepted 12th February 2015

DOI: 10.1039/c4cp05748a

www.rsc.org/pccp

Introduction

Due to their particular electronic properties, conjugated quinoidal species are attractive components in molecular electronics and optoelectronic devices for a wide range of applications. For instance, due to their good transport properties, quinone-based semiconductor channels are used in field effect transistors.¹ Although quinoidal species have emerged as promising n-channel actuators, some thiophene-based derivatives exhibit ambipolar behaviour, which meets the key requirement for complementary circuits. For longer homologues, effective π -conjugation along the planar molecular skeleton leads to low energy gap values with absorption in the red or near-infrared regions. In this regard, 5,5'-bis(3,5-di-*tert*-butyl-4-oxo-2,5-cyclohexadiene-1-ylidene)-2,2'-dihydroxy bithiophene (**QBT**, Fig. 1) has been used as a hole donor in an organic photodetector² for polymer optical fibers, which work at 650 nm.² In organic photovoltaic cells, the addition of a small quantity of **QBT** to bulk heterojunctions of P3HT:PCBM (poly-3-hexylthiophene:fullerene) resulted in a 47% increase in EQE with respect to the corresponding cells based on a P3HT:PCBM binary blend only.³ In fact, the quinoidal

species improve the non-optimal microstructure of the active layer by affecting the crystallinity of the polymer as well as the morphology of the blend.

In some conjugated quinones, the occurrence of unexpected electronic structures has been known for a long time. Thiele's⁴ and Chichibabin's⁵ hydrocarbons are the first examples of systems characterized by a biradicaloid ground state, as proven by both spectroscopic analysis and theoretical modeling.⁶ Several further series of Chichibabin-type compounds with dicyanomethylene,⁷ oxocyclohexadienylidene^{8,9} or imidazolylidene¹⁰ end groups have then been synthesized. It has been observed that molecules with a rather short sequence of conjugated units exhibit a quinoidal structure, whereas a diradical contribution occurs when increasing the conjugation length. Kozaki *et al.* reported no diradical character for **1**¹¹ and diradical participation in *cis-trans* isomerisation for **2**¹⁰ (see Fig. 1).

Using Raman spectroscopy and quantum chemical modelling, Navarrete *et al.* demonstrated the occurrence of a diradical structure in dicyanomethylene-end-capped quinoidal oligomers when the number of thiophene rings is equal to or larger than four (**3**, Fig. 1).⁷ Further Raman spectroscopy and computational studies have clearly highlighted the peculiar ground-state structure of **QBT**.¹² In the same work, Fazzi *et al.* identified the spectroscopic signature, *i.e.* the frequency position of a Raman marker band, of the biradical structure for these thiophene-based heterophenoquinone homologues.

More recently, it has been found that electron-donating alkoxy groups on the thienylene core of the 5,5'-bis-(3,5-di-*tert*-butyl-4-oxo-2,5-cyclohexadiene-1-ylidene)-3,3'-dipentoxy-2,2'-dihydroxy bithiophene (**QOO**) provide a strong contribution to the stabilization of

^a Dipartimento di Chimica, Materiali e Ingegneria Chimica, Politecnico di Milano, p.za Leonardo da Vinci 32, Milan, Italy. E-mail: chiara.bertarelli@polimi.it; Fax: +39 0270638173

^b INAF, Osservatorio Astronomico di Brera, via Bianchi 46, 23807 Merate, Italy

^c Center for Nanoscience and Technology@PoliMi, Istituto Italiano di Tecnologia, via Pascoli 70/3, Milan, Italy

† Electronic supplementary information (ESI) available. CCDC 1029034. For ESI and crystallographic data in CIF or other electronic format see DOI: 10.1039/c4cp05748a

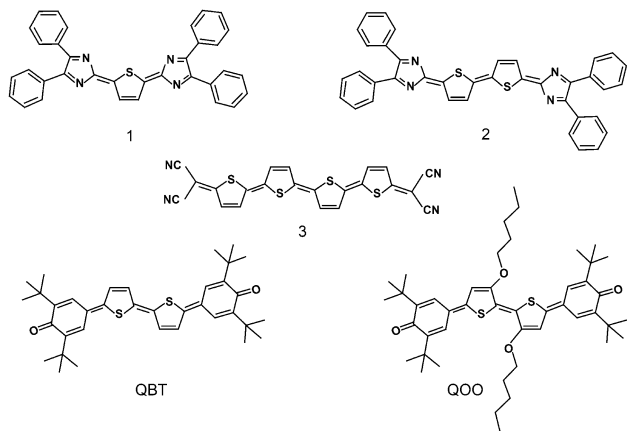


Fig. 1 Thiele's and Chichibabin's hydrocarbon analogues and heterophenoquinones.

the quinoidal ground-state structure of these species.¹³ This allows tuning of their electronic character without significantly affecting the HOMO–LUMO energy gap.

In the present study, we provide evidence of the possibility of modulating a quinoid vs. biradicaloid structure within thiophene-based heteroquaterphenoquinones bearing electron-active substituents either on the phenoquinone or on the central core.

We take **QBT** as a reference molecule, as it is the shortest molecule exhibiting a transition from a quinoidal to a biradicaloid electronic ground state among thiophene-based heterophenoquinones.¹² We demonstrate that the stabilisation of a given electronic structure depends on the nature and strength of electron-active substituents and that donor and acceptor groups provide opposite effects. Interestingly, the quinoidal vs. biradicaloid character is also affected by the position of the substituents.

Results and discussion

Materials

In oligoarylenes, as in other conjugated species, the introduction of electron-donating or electron-withdrawing substituents is known to affect the position of the frontier energy levels and their energy gap. To highlight the role of functional groups in unsaturated phenoquinones, we have introduced different substituents onto the backbone of 5,5'-bis(3,5-di-*tert*-butyl-4-oxo-2,5-cyclohexadiene-1-ylidene)-2,2'-dihydroxy bithiophene (**QBT**). The sites that we have taken into consideration for the introduction of electron-donating and electron-withdrawing groups are:

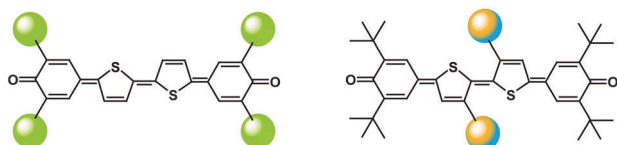


Fig. 2 General structure of the two classes of molecules: “substituted wings” (on the left) and “substituted core” (on the right). The spheres correspond to the donating or withdrawing groups introduced onto the pristine backbone.

- the 3,3'-positions of the central bithienylene core (“substituted core”, see Fig. 2, on the right). We have avoided functionalization of the 4,4'-positions since this can hamper coupling of the core with the lateral phenols due to steric hindrance;

- the lateral 4-oxo-2,5-cyclohexadiene-1-ylidene at the 3,5-positions, replacing the *t*-butyl groups (“substituted wings”, see Fig. 2, on the left). Again, substitution in these positions is preferred to the 2,6-positions, in order to avoid steric hindrance during Suzuki coupling.

All the quinoidal molecules were obtained by oxidation of their corresponding aromatic precursors. Throughout this paper, molecules are labelled with acronyms where the first letter indicates an aromatic (A) or quinoidal (Q) species. The remaining letters refer to the substituents.

The general scheme for producing the “substituted core” class (Fig. 3) follows the procedure used for **QBT**, consisting of Suzuki coupling between 5,5'-dibromo-2,2'-bithiophene and a boron derivative of the substituted phenol (**5**).¹²

3,3'-Dipentoxo-2,2'-bithiophene (**11**) was synthesized according to ref. 14 and further brominated with NBS in DMF. For 3-methoxy-2,2'-bithiophene, Kumada coupling between 2-bromo-3-methoxythiophene with NBS and the Grignard reagent of 2-bromothiophene was carried out (Scheme 1).

Suzuki coupling between the dibrominated cores and the boronic derivative **5** gave aromatic compounds, which were subsequently oxidized with potassium ferricyanide to provide **QOO** and **QHO** in quantitative yields. As the symmetrically substituted bithiophene **AOO** tends to oxidize spontaneously upon air exposure, both aromatic and quinoidal products were obtained from the workup of the reaction.

As for electron-poor **QBT** derivatives, two electron-withdrawing groups have been considered, namely 1,3-dioxolane (**QXX**) and carboxylic acid (**QCO**). These two species were obtained in succession *via* the same synthetic route. In the latter case, the carboxylic group was obtained in the last oxidation step, starting from aldehyde groups in the 3,3'-positions. The synthetic route is reported in Scheme 2.

The two dibrominated bithienylene cores (**16** and **18**) were synthesized almost entirely following the published procedure.¹⁵ According to the original route, 5,5'-dibromo-3,3'-diformylacetal-2,2'-bithiophene (**16**) was not isolated, but it was directly deprotected. Herein, the cleavage of **16** was not carried out in a one-pot reaction.

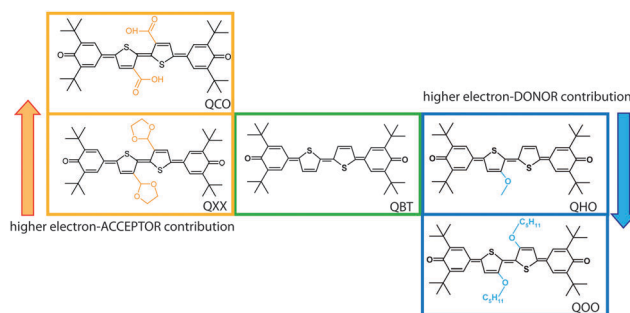
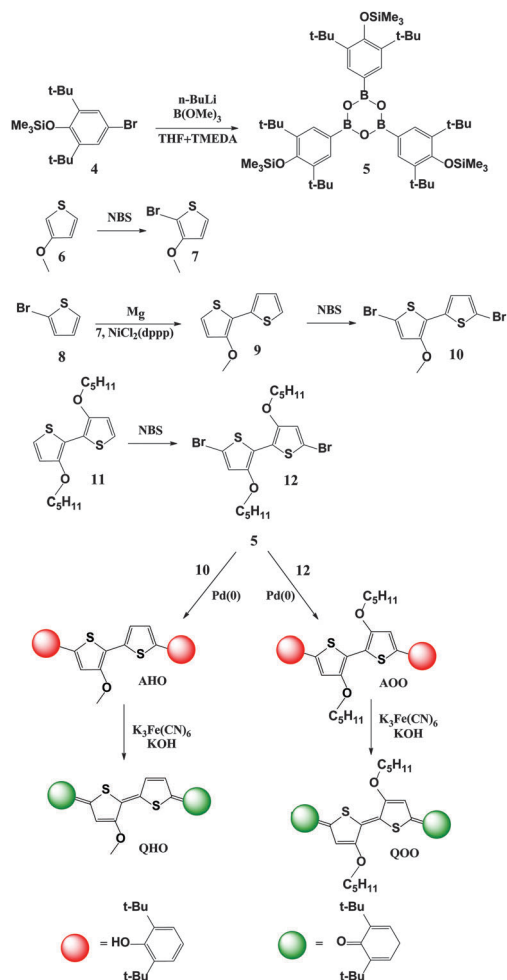


Fig. 3 “Substituted core” class of quinoidal molecules starting from **QBT**: **QCO**, **QXX**, **QHO**, **QOO**.

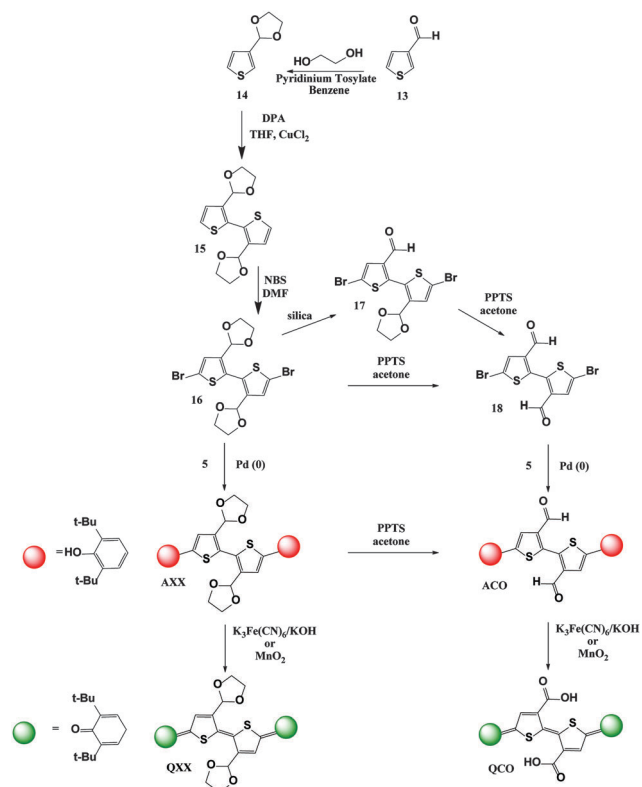


Scheme 1 Synthetic route to the quinones belonging to the "substituted core" class bearing donor groups.

Accordingly, compound **16** was isolated before proceeding to the next deprotection step. Incidentally, it was found that bromination of **15** did not only provide **16**, which is white-coloured, but also a yellow product, which proved to be 5,5'-dibromo-3'-(1,3-dioxolan-2-yl)-[2,2'-bithiophene]-3-carbaldehyde (**17**), due to partial deprotection of **16** on silica. Suzuki coupling between the dibrominated cores (**16** or **18**) and the boronic derivative (**5**) gave the aromatic compounds **AXX** and **ACO**. 5,5'-Bis(3,5-di-*tert*-butyl-4-hydroxyphenyl)-[2,2'-bithiophene]-3,3'-dicarbaldehyde (**ACO**) was also obtained through deprotection of the diformylacetal groups of **AXX** with pyridinium tosylate (PPTS) in acetone (Scheme 2).

It is well known that introduction of electron-acceptor groups induces an increase in oxidation potential in π -conjugated systems, and hence hampers chemical and electrochemical oxidative reactions. Therefore, unlike the case of **AOO**, where the oxidation step proceeds spontaneously, oxidation of aromatic precursors substituted with acceptor groups has been shown to be more difficult. In addition to potassium ferricyanide, MnO_2 has also been tested as an oxidizing agent. The latter has allowed recovery of the desired products in quantitative yields.

The set of "substituted wings" compounds is obtained by replacement of the *t*-butyls in the α,α' -positions on the phenols



Scheme 2 Synthetic route to the quinones belonging to the "substituted core" class bearing withdrawing groups.

of the **QBT** structure with electron-active groups, leaving the central bithienylene core unchanged (Fig. 4).

Two different synthetic strategies were followed. The first one employed Suzuki coupling, starting from a lateral *p*-brominated phenol and a diboronated bithienylene core. This route was applied with a phenol substituted with electron-donating groups,

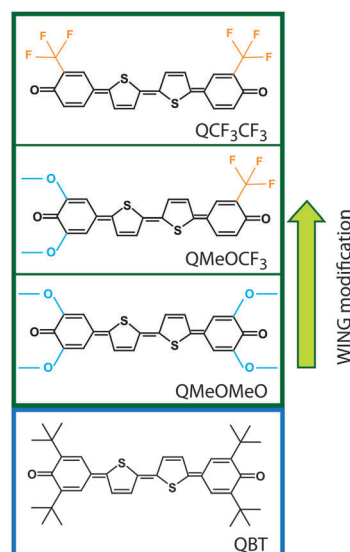
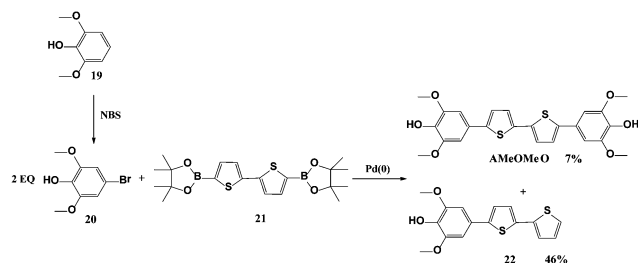


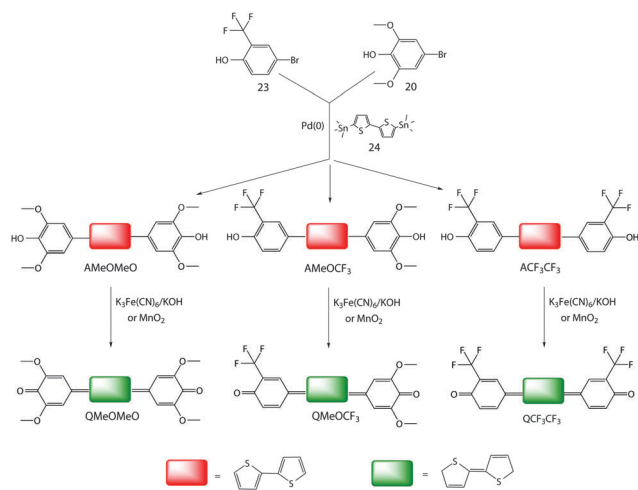
Fig. 4 "Substituted wings" class of quinoidal molecules starting from **QBT**: **QMeOMeO**, **QMeOCF₃**, and **QCF₃CF₃**.

Scheme 3 Suzuki coupling for the synthesis of **AMeOMeO**.

4-bromo-2,6-dimethoxyphenol (**20**), and a pinacol ester of 2,2'-bithiophene (**21**) (Scheme 3).

This reaction gave the desired product in very low yields, with the monosubstituted compound (**22**) as the main product. Since Stille coupling between 5,5'-bis(trimethylstannyl)-2,2'-bithiophene (**24**) and **20** (Scheme 4) provided higher yields than the Suzuki reaction, the same route was applied to the synthesis of both the other molecules bearing substituted wings (*i.e.* **ACF₃CF₃** and **AMeOCF₃**). Runs were also repeated under microwave irradiation, but no significant advantage was observed.

The asymmetrical **AMeOCF₃**, which contains both a donor-substituted wing at one end and an acceptor-substituted wing at the other end, required optimization of the experimental conditions to avoid or limit the formation of the symmetrically substituted molecules as main products (*i.e.* **AMeOMeO** and



Scheme 4 Synthetic route to yield "substituted wings" quinoidal molecules.

Table 1 Runs aimed at determining the correct timing of introduction of the two different wings to obtain **AMeOCF₃**

Run	Addition time ^a		Yields (%)		
	20 ^b	23 ^b	AMeOMeO	AMeOCF₃	ACF₃CF₃
1	After 45	0	0	0	43
2	0	After 25	34	0	0
3	0	0	4	34	9.5

^a In minutes. ^b Phenol derivatives used as reactants.

ACF₃CF₃). It was found that, with simultaneous introduction of the two different phenols (Run 3 in Table 1), the asymmetrical molecule **AMeOCF₃** is recovered as the main product (34%), whereas the symmetrical species are formed in lower yields (4% and 9.5% for **AMeOMeO** and **ACF₃CF₃**, respectively).

All the aromatic compounds were oxidized to the corresponding quinones using either MnO_2 or potassium ferricyanide, the latter facilitating the following purification step. This oxidant is in fact soluble in the reaction medium whereas the desired products precipitate, thus allowing for their easy separation by filtration.

Absorption and fluorescence spectroscopy of aryls (A) and quinones (Q)

UV-vis spectroscopy is a convenient method to highlight the strong change in π -delocalisation when passing from an aromatic to a quinoidal structure. The peculiar absorption of quinoidal species at low energy is due to the almost double inter-ring bond that forces the skeleton into a more planar conformation, leading to a loss of aromatic character and more extended π -delocalisation.

Except for **QOO** and **QCF₃CF₃**, the UV-vis spectra of these quinoidal species show the same features as the reference **QBT**

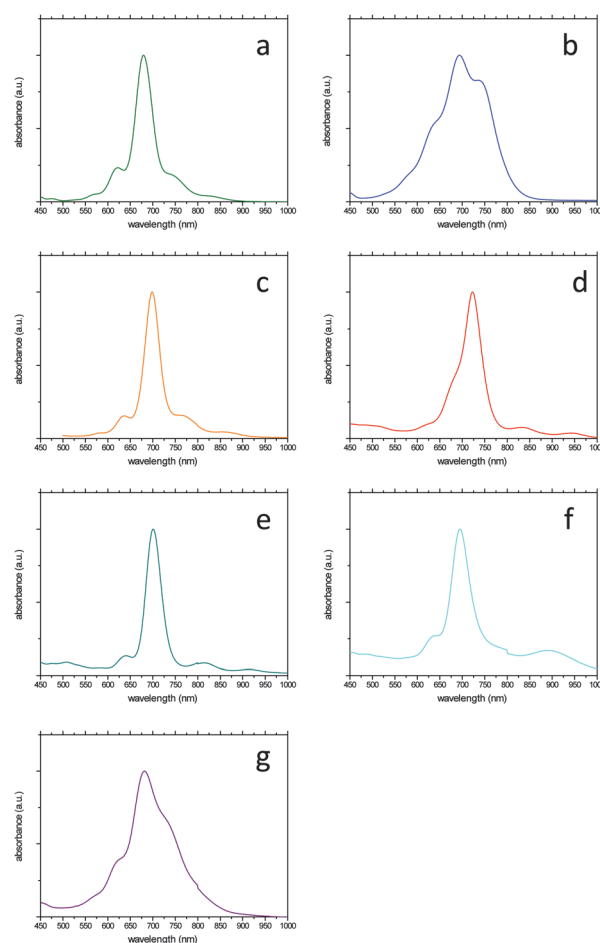


Fig. 5 Normalized absorption spectra of "substituted core" and "substituted wings" species in chloroform: (a) **QBT**, (b) **QOO**, (c) **QXX**, (d) **QCO**, (e) **QMeOMeO**, (f) **QMeOCF₃**, (g) **QCF₃CF₃**.

(Fig. 5). In fact, the functionalized quinones exhibit a sharp, very intense band assigned to the strongest dipole-allowed transition, with a defined vibronic structure, at higher energy and a weaker transition, which has been previously assigned to a weak double-electron excitation, at lower energy.¹⁶

The change in π -conjugation going from aromatic precursors to the corresponding quinones can be highlighted by the strong red-shift of the absorption bands (see Δ red shift in Table 2). This shift is the largest for **XX**, which is characterized by a distorted backbone in the aromatic form (**AXX**). In fact, the presence of bulky substituents on the 3,3'-positions of the bithiophene causes a deviation from planarity through rotation about the quasi-single thiophene-thiophene inter-ring bond. Relative to unsubstituted **ABT**, a remarkable blue-shift in the π - π^* transition is observed when acceptor groups are introduced into the bithiophene (**AXX**, **ACO**). In **ACO**, together with the main absorption band at 270 nm, a weaker band at 406 nm is present, which is ascribed to an n - π^* transition (see ESI[†]), in analogy with other aromatic structures containing carbonyl groups.

Conversely, the smallest shift of the main absorption band going from an aromatic precursor to the corresponding quinone is displayed by a "substituted core" species bearing an alkoxy group (Δ red shift = 290 nm). Introduction of this substituent into the core of the molecule provides a relevant donor contribution to the aromatic backbone through a resonance effect without causing significant distortion.¹⁷ This effect also plays a significant role in the case of aromatic compounds, as shown by the red-shift of the absorption maximum of **AOO** (406 nm) with respect to **ABT** (382 nm). Planarization in both **AOO** and **QOO** is likely related also to a stabilizing oxygen-sulphur interaction, which adds to the contribution of the resonance forms, which are expected to counterbalance any sterically induced distortion effect.¹⁸

An indication of the degree of planarity of the molecular skeleton for the aromatic species is also given by the Stokes shift values. The photoluminescence spectra of **ABT** and **AOO** are characterized by a well-defined vibronic structure with an energy separation of about 0.15 eV (spectra are reported in the ESI[†]). The presence of the vibronic structure in the emission can be ascribed to planarization of the molecular skeleton triggered by the excitation.¹⁹ The Stokes shift values are in the typical range for a linear conjugated oligomer²⁰ and decrease with an increase in planarization along the conjugated skeleton, as in the case of **AOO** (0.38 eV, see ESI[†]). Conversely, the photoluminescence spectrum of **ACO** is characterized by a roughly defined vibronic structure shifted to longer wavelength, whereas **AXX** does not display any vibronic shoulder and has a large Stokes shift (1.00 eV), which is ascribed to the large variation in equilibrium geometry between the ground and excited states.

According to all the reported data, for the "substituted core" species planarization of the skeleton in the quinoidal structure counteracts the hindrance effect of the side groups, which is relevant in the aromatic precursors instead.

As a result of the electronic effect of the substituents, the absorption maxima of **QOO**, **QXX** and **QCO** are red-shifted with respect to **QBT**. Comparison between the three different "substituted wings" species (*i.e.* **QMeOMeO**, **QMeOCF₃**, and **QCF₃CF₃**) highlights

Table 2 Absorption maxima of aromatic (**A-molec**) and quinoidal (**Q-molec**) compounds in chloroform solution. The extinction coefficient values ϵ ($M^{-1} cm^{-1}$) are reported in brackets. The red-shift going from aromatic to quinoidal species is also highlighted

Compound	A-molec λ_{max} (nm)	Q-molec λ_{max} (nm)	Δ red-shift (nm)
BT	382 (37 000)	680 (205 000)	299
OO	406 (26 000)	696 (100 000)	290
XX	329 (21 000)	699 (96 000)	370
CO	270–406 (25 000–9460)	722 (111 000)	316
MeOMeO	385 (19 000)	702 (191 000)	317
MeOCF₃	379 (20 000)	695 (89 000)	316
CF₃CF₃	372 (18 000)	680 (85 000)	308

the strongest effect in the methoxy-substituted quinones and the weakest one in the molecule with the $-CF_3$ acceptor groups. The shift in absorption bands when going from aromatic to quinoidal species (Δ red shift, Table 2) is similar for all three compounds and indicates that the introduction of donating and withdrawing groups onto the lateral phenol does not cause any significant distortion of the backbone. This is also confirmed by the relatively low Stokes shift values (between 0.46 and 0.50 eV, see ESI[†]), which are comparable to that of **ABT**. These pieces of evidence indicate that not only is the conjugated backbone not distorted by the introduction of substituents, but also their electronic effect is negligible.

Surprisingly, the donor-acceptor quinone (**QMeOCF₃**) displays an intermediate effect with respect to the symmetrically substituted **QMeOMeO** and **QCF₃CF₃**. This behaviour suggests that no cross-talk occurs between the electron-active groups and therefore no push-pull species is actually formed. None of the quinones described here exhibit any fluorescence.

The role of functional groups in changing the electronic character: quinoidal vs. biradicaloid ground state

Despite controversial views regarding the correct description of the ground-state electronic structure of conjugated quinones, previous works have highlighted the strict relationship between diradicals and π -conjugation along the backbone in the homologous series of thiophene-based heterophenquinones.¹² In this respect, Raman-active modes are a powerful tool for discriminating between different π -conjugated compounds on the basis of their characteristic fingerprints. In particular, the so-called \mathcal{A} -mode, which corresponds to oscillation of the bond length alternation (BLA) parameter relative to the CC sequence along a conjugated structure,^{2,21} gives strong, diagnostic marker bands. As reported in our previous work,¹² the Raman frequency of the \mathcal{A} -mode of **QBT**, at $1304 cm^{-1}$, is unusually low with respect to the \mathcal{A} frequency commonly exhibited by aromatic oligothiophenes and short thienoquinoid oligomers, which is observed at about $1440 cm^{-1}$. This feature is a clear signature of the biradicaloid structure of **QBT**. Indeed, the remarkable downward shift of the \mathcal{A} -mode can be rationalized only by considering an almost "equalized" CC bond sequence in the bithiophene moiety, as predicted by density functional theory calculations adopting a broken-symmetry (BS) wavefunction.¹² Conversely, not only does the most common closed-shell (CS) approach predict a quinoidal equilibrium structure for **QBT**, but it also

provides a computed Raman spectrum showing the usual \mathcal{A} -mode band at about 1400 cm^{-1} , in total disagreement with the experimental observation.

According to these previous studies,^{12,13} we expect that fine-tuning of the ground-state electron charge distribution by the introduction of electroactive substituents into the **QBT** skeleton results in a remarkable modulation of the Raman features. Being specifically used as a diagnostic tool to determine a possible diradical contribution to the ground state of conjugated quinones, Raman spectroscopy was carried out only for the **Q**-molecules studied here and not for the **A**-species which do not exhibit this particular electronic character. Direct comparison of the experimental Raman fingerprints allows us to classify these quinones without any support from theoretical modelling of the spectra, as the conjugated skeleton is the same for all the substituted species discussed here.

As previously reported, the Raman spectrum of **QOO** is markedly different from that of unsubstituted **QBT**, displaying the strongest band, which is assigned to the \mathcal{A} -mode, at 1430 cm^{-1} , up-shifted by more than 100 cm^{-1} with respect to the \mathcal{A} -mode transition of the biradicaloid species (Fig. 6).¹³ The presence of a strong line assigned to the \mathcal{A} -mode at higher energy proves that the dialkoxy-substituted phenoquinone is described by a quinoidal ground state. Given this first result, the next step was to investigate whether the effect of functional groups at the 3,3'-positions of the bithienylene core ("substituted core") is unequivocal in stabilizing a quinoidal ground state or depends on their specific electronic character (*i.e.* donor or acceptor).

QXX and **QCO** exhibit several spectral features comparable to those of **QBT** (Fig. 6). For **QXX** and **QCO**, the strongest bands are at 1230 cm^{-1} and 1130 cm^{-1} , respectively, down-shifted by $\sim 200\text{--}300\text{ cm}^{-1}$ with respect to the \mathcal{A} -mode transition characteristic of the quinoidal species discussed above (**QOO**).

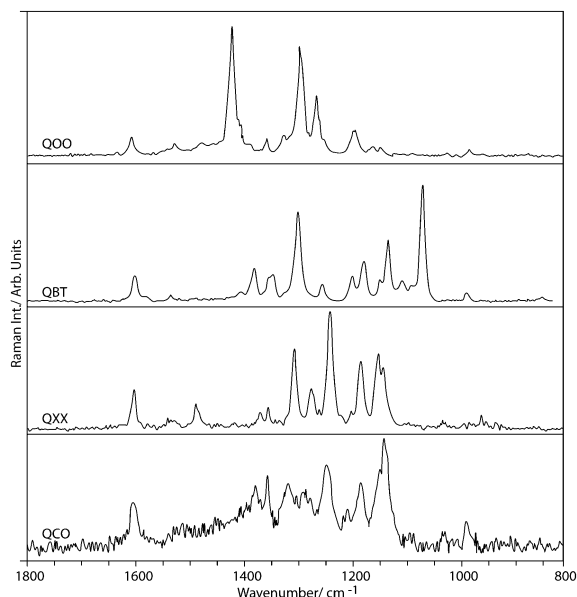


Fig. 6 Raman spectra of powder samples of (see labels on the left): **QOO** (FT-Raman) and **QBT**, **QXX**, and **QCO** (excitation line: 632 nm).

Since the position of the \mathcal{A} -mode is directly related to the molecular structure and it is red-shifted in the presence of a biradicaloid character, it is possible to assign a biradicaloid geometry to **QXX** and **QCO**.

It turns out that modification of the electron distribution in a thiophene-based quaterphenoquinone by means of electroactive substituents on the conjugated core leads to stabilization of a quinoidal ground state only when donor groups are introduced. Acceptor groups likely provide the opposite effect.

QBT and **QMeOMeO** exhibit similar Raman spectra: considering the spectral region $1800\text{--}900\text{ cm}^{-1}$, the most intense peak is located at $\sim 1300\text{ cm}^{-1}$ (Fig. 7). As demonstrated before for **QBT**,¹² the anomalous low frequency of the \mathcal{A} -mode can be explained only by taking into account a biradicaloid ground-state character. The similarity in the main Raman features between the **QBT** and **QMeOMeO** spectra further establishes the fact that **QMeOMeO** has a ground state with a biradicaloid nature.

Conversely, **QCF₃CF₃**, which is characterized by withdrawing substituents on the phenones, strongly differs from **QBT**, while being more similar to **QOO**: its Raman spectrum exhibits the strongest band, assigned to the \mathcal{A} -mode, at $\sim 1430\text{ cm}^{-1}$, which indicates, for this molecule, a quinoidal ground state (Fig. 7).

This evidence leads to the conclusion that the introduction of electron-active substituents on the lateral phenones has the opposite effect on the electronic behaviour of these materials, compared to the introduction of electron-donating/withdrawing groups onto the central core. In other words, it has been demonstrated that the electronic character of functionalized **QBTs** in the ground state depends not only on the nature of the electron-active substituents, but also on their position on the main backbone. This is likely related to diradical delocalization over the molecular structure.

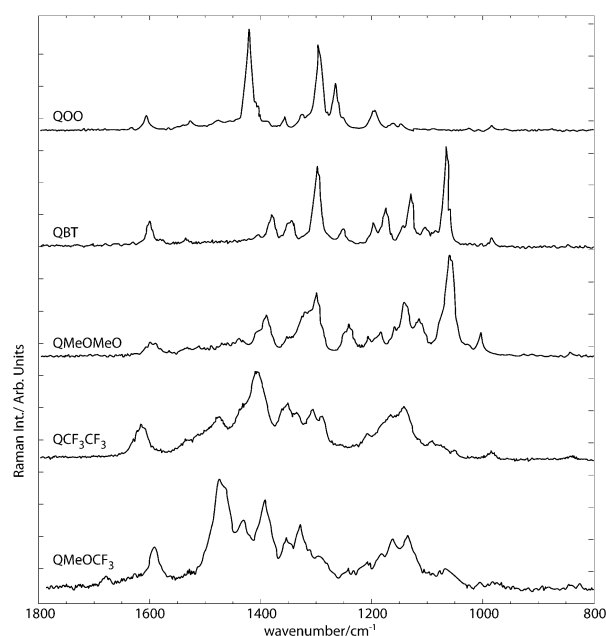


Fig. 7 Raman spectra of powder samples of (see labels on the left): **QOO** (FT-Raman) and **QBT**, **QMeOMeO**, **QCF₃CF₃**, and **QMeOCF₃** (excitation line: 632 nm).

QMeOCF₃ exhibits the strongest band delocalized at a lower wavelength, $\sim 1470\text{ cm}^{-1}$, suggesting higher stability of the quinoidal configuration. The donor-acceptor strategy, which generally plays a significant role in modifying the electron distribution in aromatic oligomers, thus giving low-band-gap materials, is not effective in the case of conjugated phenoquinones. As a consequence, since π -conjugation does not increase, a biradicaloid ground state is not obtained.

Crystal structure

Among all the quinones presented here, it was possible to collect a full X-ray diffraction data set only for **QOO**. This class of thiophene-based heterophenoquinones does not usually provide single crystals of sufficient quality for X-ray data collection and, to date, only the crystal structure of 2,5-bis-(3,5-di-*tert*-butyl-4-oxo-2,5-cyclohexadiene-1-ylidene)-1,5-dihydrothiophene has been reported.²² However, for conjugated quinones, X-ray structure investigation may also provide further validation of the results obtained by Raman analysis. From the XRD data of **QOO**, the occurrence of a mainly quinoidal molecular structure, exhibiting alternate shorter and longer CC bonds according to the pattern established by the phenoquinone ends, is expected.

Small dark green needles were grown by slow evaporation from a toluene solution of **QOO** at 4 °C. A summary of the major crystallographic data is reported in the ESI.† Data collection was carried out at room temperature. Despite the thin plate-like morphology of the crystals, a complete X-ray diffraction data set could be collected and the structure unambiguously determined and fully refined anisotropically. No clear diffraction was observed beyond the 2θ value at which the structure is reported. Further attempts to improve the three-dimensional size and quality of the crystals were unsuccessful, most likely owing to intrinsic structural features of the molecule. Overall,

the structure confirms the high degree of planarity of the molecule (Fig. 8).

Only half a molecule is present in the asymmetric unit, the other half being generated through an inversion centre. The two phenyl rings are essentially coplanar with the core, the C(3)–C(4)–C(5)–C(10) torsion angle being 2.6° . Further contributions to the planarity of the system are interactions between the oxygen and sulphur atoms within the central moiety of the molecule. In fact, the distance between the sulphur atom and the oxygen of the pentoxy group is 2.8 Å. The two pentoxy groups slightly extend above and below the plane of the molecule (see Fig. 8b). As expected, the outermost C atoms in the pentoxy groups exhibit a large vibrational motion, suggesting a low degree of packing constraint.

A close check of the bond distance distribution in the molecule (Table 3) shows clear differences within the phenone moiety that confirm the dearomatization process that occurs in going from aromatic precursors to quinoidal species. Moreover, the bond length distribution along the skeleton clearly suggests

Table 3 Bond lengths and angles in **QOO**

Bond distance (Å)	
O(2)–C(8)	1.247 (9)
C(8)–C(7)	1.482 (11)
C(9)–C(8)	1.472 (11)
C(7)–C(6)	1.376 (10)
C(9)–C(10)	1.350 (10)
C(5)–C(6)	1.426 (10)
C(10)–C(5)	1.432 (10)
C(5)–C(4)	1.408 (10)
C(4)–C(3)	1.414 (10)
C(2)–C(3)	1.364 (10)
C(1)–C(1)	1.409 (14)
C(1)–C(2)	1.420 (10)
Angle	
C(4) C(5) C(6)	121.4 (8)
C(3) C(4) C(5)	128.5 (7)
Torsion angle	
C(3) C(4) C(5) C(10)	177.6 (8)
C(6) C(5) C(4) S(1)	(–) 178.8 (6)

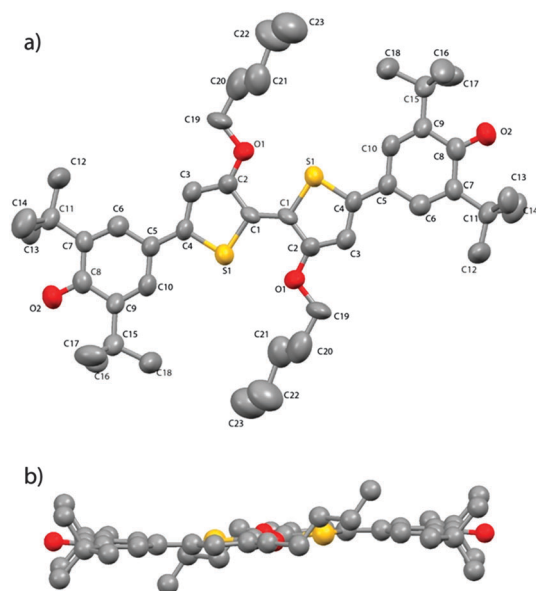


Fig. 8 Molecular structure of **QOO**: (a) top view and (b) side view.

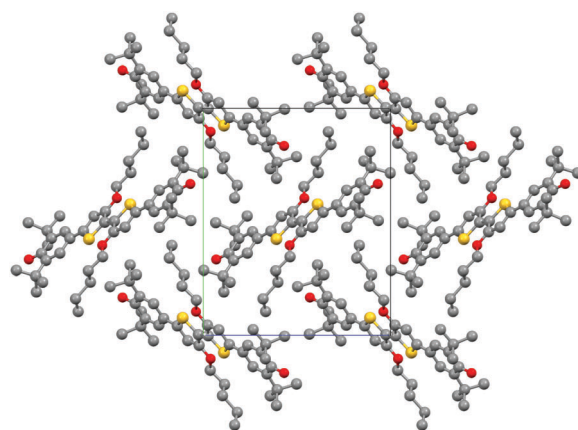


Fig. 9 Crystal structure of **QOO** viewed along the *a*-axis.

a quinoidal electronic character, as expected. Interestingly, the formal inter-ring double bonds C(1)–C(1) and C(4)–C(5) are longer than the intra-ring double bonds, namely C(2)–C(3), C(6)–C(7) and C(9)–C(10).

No π – π stacking interaction is observed in the crystal (Fig. 9).

Short intermolecular contact distances of 3.6 Å between *t*-butyl moieties belonging to nearest neighbouring molecules stabilize the molecular packing arrangement in the crystal. Further C–H... π stabilizing contacts between *t*-butyls and centroids of thiophene rings are also observed. These interactions can contribute to stabilization of the observed crystal packing arrangement, which is characterized by the presence of large cavities.

Conclusion

New thiophene-based quaterphenoquinones with separate control over the band gap and the quinoid vs. biradicaloid structure have been investigated by introducing electron-active substituents both onto the lateral phenoquinones and the central core.

Theoretical prediction of the Raman spectra allowed clear identification and rationalization of the spectroscopic markers that can be taken as signatures of a transition from a quinoidal to a biradicaloid structure as a result of suitable chemical modifications. Specifically, it was demonstrated that the presence of donor or acceptor groups on the central moiety produced opposite effects on the stabilization of the electronic character of the structure in the ground state. The reverse occurs when the substituents are placed on the lateral phenones, suggesting that donor groups at the 3,3'-positions of the bithiophene central core stabilize a quinoidal ground state, whereas a biradicaloid electronic structure results from introduction of the same donor groups onto the lateral wings.

Finally, the simultaneous presence of donor and acceptor groups at opposite ends of the molecule does not reduce the energy gap and therefore does not significantly affect the π -conjugation. The strength of a withdrawing trifluoromethyl group prevails over the donation of electronic charge from an alkoxy group, thus resulting in a quinoidal ground state.

Experimental section

Synthesis

Unless otherwise specified, all reagents, catalysts, spectroscopic-grade and reagent-grade solvents were commercial (Sigma Aldrich). All reactions of air- and water-sensitive reagents and intermediates were carried out in dried glassware and an argon atmosphere. Solvents were previously dried by conventional methods and stored under argon. Air- and water-sensitive solutions were transferred with hypodermic syringes or *via* a cannula.

3-Thiophenecarboxaldehyde acetal (14). To a solution of 3-thiophenecarboxaldehyde (13) (10.0 g, 89.17 mmol) in benzene (100 mL) were added 1,2-ethanediol (20 mL) and pyridinium *p*-toluenesulfonate (4.1 g). The resulting mixture was refluxed with water separation by a Dean–Stark trap until the starting

aldehyde was completely reacted (*ca.* 6 h). The solvent was removed under reduced pressure, diethyl ether was added and the crude product was washed with sodium hydrogen carbonate solution and saturated sodium chloride solution. The organic phase was dried with sodium sulfate, the solvent was removed under reduced pressure and the residue was distilled (3×10^{-1} mbar, 55 °C) to give 10.5 g of the desired product in 75% yield.

¹H-NMR (400 MHz, CDCl₃): δ = 7.42 (dd, J (H,H) = 3.15 Hz, 4J (H,H) = 0.92 Hz, 1H; Th-H₂), 7.32 (dd, J (H,H) = 3.15 Hz, 4J (H,H) = 5.08 Hz, 1H; Th-H₅), 7.18 (dd, J (H,H) = 3.15 Hz, J (H,H) = 5.08 Hz, 1H; Th-H₄), 5.91 (s, 1H; O–CH–O), 4.08 ppm (dm; CH₂–CH₂).

3,3'-Diformylacetal-2,2'-bithiophene (15). *n*-Butyllithium (12 mL, 30 mmol, 2.5 M in hexane) was added dropwise to a stirred solution of diisopropylamine (2.90 g, 28.7 mmol) in 25 mL dry THF at –78 °C under an argon atmosphere. After 120 minutes, 3-thiophenecarboxaldehyde acetal (14) (4.50 g, 28.7 mmol) in 35 mL dry THF was added dropwise; the resulting mixture was stirred at a low temperature for a further 30 minutes. Then 4.50 g anhydrous CuCl₂ was added in one portion and the reaction bath was allowed to warm up to room temperature and stirred overnight. The reaction mixture was poured into water and extracted with CH₂Cl₂. The organic phase was washed, dried over MgSO₄ and evaporated under reduced pressure. The raw product was purified by flash chromatography (silica gel, 8 : 2 petroleum ether : ethyl acetate) and recrystallized from petroleum ether/CH₂Cl₂ (8 : 2), to afford 1.99 g (45%) of the title product as a white crystalline solid.

¹H-NMR (400 MHz, CDCl₃): δ = 7.36 (d, 3J (H,H) = 5.44 Hz, 2H; Th-H₅, H_{5'}), 7.21 (d, 3J (H,H) = 5.44 Hz, 2H; Th-H₄, H_{4'}), 5.72 (s, 2H; O–CH–O), 4.11 (m, 4H; acetal), 3.93 ppm (m, 4H; acetal).

5,5'-Dibromo-3,3'-diformylacetal-2,2'-bithiophene (16). NBS (3.57 g, 20.0 mmol) was added portionwise to a stirred solution of 3,3'-diformylacetal-2,2'-bithiophene (3.11 g, 10.0 mmol) in freshly distilled DMF (15 mL) at room temperature in the dark. The suspension was stirred for 5 hours until the reaction was complete, poured onto ice and extracted with diethyl ether. The combined organic layers were dried over Na₂SO₄, filtered and the solvent was removed under reduced pressure. The raw product was purified using flash chromatography (silica gel, 8 : 2 petroleum ether : ethyl acetate) to afford 2.30 g (48% yield) of the desired product as a pale yellow crystalline solid.

¹H-NMR (400 MHz, CDCl₃): δ = 7.16 (s, 2H; Th-H₄, H_{4'}), 5.66 (s, 2H; O–CH–O), 4.089 (m, 4H; acetal), 3.94 ppm (m, 4H; acetal).

1.50 g of a yellow powder was also obtained, which corresponds to the asymmetrical deprotected product, 5,5'-dibromo-3'-(1,3-dioxolan-2-yl)-[2,2'-bithiophene]-3-carbaldehyde (17). ¹H-NMR (400 MHz, CDCl₃): δ = 9.70 (s, 1H; CHO), 7.49 (s, 1H; Th-H), 7.23 (s, 1H; Th-H), 5.61 (s, 1H; O–CH–O), 4.06 (m, 2H; acetal), 3.94 ppm (m, 2H; acetal).

5,5'-Dibromo-3,3'-diformyl-2,2'-bithiophene (18)

Method A. A solution of 5,5'-dibromo-3,3'-diformylacetal-2,2'-bithiophene (2.25 g, 4.8 mmol) in 120 mL acetone containing pyridinium tosylate (PPTS) (1.05 g) was refluxed until the reaction was complete (usually 2 days, thin layer test). The solvent was then removed under reduced pressure and the residue was dissolved in CH₂Cl₂ and washed with sodium hydrogen carbonate solution and

saturated sodium chloride solution. The organic phase was dried and evaporated to give the title product in quantitative yield.

Method B. A solution of 5,5'-dibromo-3'-(1,3-dioxolan-2-yl)-[2,2'-bithiophene]-3-carbaldehyde (2.00 g, 4.72 mmol) in 100 mL acetone containing pyridinium tosylate (PPTS) (600 mg) was refluxed until the reaction was complete (usually 2 days, thin layer test). The solvent was then removed under reduced pressure and the residue was dissolved in CH₂Cl₂ and washed with sodium hydrogen carbonate solution and saturated sodium chloride solution. The organic phase was dried and evaporated to give the title product in quantitative yield.

¹H-NMR (400 MHz, CDCl₃): δ = 9.75 (s, 2H; CHO), 7.58 ppm (s, 2H; Th-H₄, H₄').

4,4'-(3,3'-Di(1,3-dioxolan-2-yl)-[2,2'-bithiophene]-5,5'-diyl)-bis(2,6-di-*tert*-butylphenol) (AXX). To a solution of 5,5'-dibromo-3,3'-diformylacetate-2,2'-bithiophene (650 mg, 1.38 mmol) and Pd(PPh₃)₄ (160 mg, 0.14 mmol) in previously degassed DME (2:1 with respect to water), tris[3,5-di-*tert*-butyl-4-(trimethylsilyloxy)phenyl]boroxine (5) (1.27 mg, 1.38 mmol) and Na₂CO₃ (1.31 g, 12.4 mmol) in aqueous solution (1 M) were rapidly added. The resulting mixture was refluxed for 19 hours. Then it was allowed to cool to room temperature, poured into water and extracted with diethyl ether. The organic layers were combined, dried over Na₂SO₄ and filtered. After solvent removal, a yellow powder was obtained. The crude product was first washed with hot ethanol and then with ethyl acetate to yield 956 mg (96% yield) of the desired product as a bright yellow powder.

¹H-NMR (400 MHz, CDCl₃): δ = 7.40 (s, 4H; Ph-H), 7.25 (s, 2H; Th-H₄, H₄'), 5.77 (s, 2H; O-CH-O), 5.29 (s, 2H; -OH), 4.16 (m, 4H; acetal), 3.96 (m, 4H; acetal), 1.48 ppm (s, 36H; *t*-Bu); HRMS (ESI): *m/z* calcd for C₄₂H₅₄O₆S₂ + H⁺: 741 [M + Na⁺], found: 741.3 (M + Na⁺).

4,4'-(3,3'-Di(1,3-dioxolan-2-yl)-5H,5'H-[2,2'-bithiophenylidene]-5,5'-diylidene)-bis(2,6-di-*tert*-butylcyclohexa-2,5-dienone) (QXX)

Method A. To a solution of 4,4'-(3,3'-di(1,3-dioxolan-2-yl)-[2,2'-bithiophene]-5,5'-diyl)-bis(2,6-di-*tert*-butylphenol) (AXX) (70 mg, 0.097 mmol) in CH₂Cl₂ (24 mL), K₃Fe(CN)₆ (320 mg, 0.97 mmol) and a 0.4 M aqueous solution of KOH (546 mg, 9.74 mmol) were added. The resulting mixture was stirred until the starting material was completely reacted (≈ 2 hours). The reaction mixture was extracted with methylene chloride and washed with water and the organic solvent was removed under reduced pressure. The raw product was washed with toluene to afford 61 mg (87% yield) of QXX as an iridescent green solid.

Method B. To a solution of 4,4'-(3,3'-di(1,3-dioxolan-2-yl)-[2,2'-bithiophene]-5,5'-diyl)-bis(2,6-di-*tert*-butylphenol) (AXX) (20 mg, 0.028 mmol) in CH₂Cl₂ (8 mL), MnO₂ (17 mg, 0.190 mmol) was added. The resulting mixture was stirred until the starting material was completely reacted (≈ 2 hours 40 minutes). The reaction mixture was filtered and the organic solvent was removed under reduced pressure. The desired product was collected as an iridescent green solid in quantitative yield.

¹H NMR (400 MHz; CDCl₃): δ = 7.41 (br. s; Ph-H), 7.31 (br. s; Th-H₄, H₄'), 5.72 (s, 2H; O-CH-O), 4.25 (m, 4H; acetal), 4.15

(m, 4H; acetal), 1.42 ppm (s, 36H; *t*-Bu); HRMS (ESI): *m/z* calcd for C₄₂H₅₂O₆S₂ + H⁺: 717 [M + H⁺], found: 717.3 (M⁺).

5,5'-Bis(3,5-di-*tert*-butyl-4-hydroxyphenyl)-[2,2'-bithiophene]-3,3'-dicarbaldehyde (ACO)

Method A. To a solution of 5,5'-dibromo-3,3'-diformyl-2,2'-bithiophene (18) (500 mg, 1.32 mmol) and Pd(PPh₃)₄ (151 mg, 0.13 mmol) in previously degassed DME (2:1 with respect to water), tris[3,5-di-*tert*-butyl-4-(trimethylsilyloxy)phenyl] boroxine (5) (1.2 mg, 1.32 mmol) and Na₂CO₃ (1.25 g, 11.8 mmol) in aqueous solution (1 M) were rapidly mixed. The resulting mixture was refluxed for 18 hours. After cooling to room temperature, it was poured into water and extracted with diethyl ether. The organic layers were combined, dried over Na₂SO₄ and filtered. By solvent removal, a dark yellow powder was obtained. The crude product was washed with hexane and then with ethanol to yield 549 mg (87% yield) of the desired product as a light yellow powder.

Method B. A solution of 4,4'-(3,3'-di(1,3-dioxolan-2-yl)-[2,2'-bithiophene]-5,5'-diyl)-bis(2,6-di-*tert*-butylphenol) (AXX) (150 mg, 0.208 mmol) in 10 mL acetone containing pyridinium tosylate (PPTS) (133 mg) was refluxed for 16 hours. The solvent was then removed under reduced pressure and the residue was dissolved in DCM and washed with sodium hydrogen carbonate solution and saturated sodium chloride solution. The organic phase was dried and solvent-evaporated to give the title product in quantitative yield as a light yellow solid.

¹H-NMR (400 MHz, CDCl₃): δ = 9.93 (s, 2H; CHO), 7.66 (s, 2H; Th-H₄, H₄'), 7.44 (s, 4H; Ph-H), 5.77 (s, 2H; O-CH-O), 5.43 (s, 2H; -OH), 1.49 ppm (s, 36H; *t*-Bu); HRMS (ESI): *m/z* calcd for C₃₈H₄₆O₄S₂ + H⁺: 631 [M + H⁺], found: 629.4 (M⁺).

5,5'-Bis(3,5-di-*tert*-butyl-4-oxocyclohexa-2,5-dien-1-ylidene)-5H,5'H-[2,2'-bithiophenylidene]-3,3'-dicarboxylic acid (QCO)

Method A. To a solution of 5,5'-bis(3,5-di-*tert*-butyl-4-hydroxyphenyl)-[2,2'-bithiophene]-3,3'-dicarbaldehyde (ACO) (33 mg, 0.052 mmol) in CH₂Cl₂ (24 mL), K₃Fe(CN)₆ (172 mg, 0.52 mmol) and a 0.4 M aqueous solution of KOH (293 mg, 5.23 mmol) were added. The resulting mixture was stirred until the starting material was completely reacted (≈ 2 hours). The reaction mixture was extracted with methylene chloride and washed with water and the organic solvent was removed under reduced pressure. The raw product was washed with toluene to afford 26 mg (84% yield) of QCO as an iridescent dark green/red solid.

Method B. To a solution of 5,5'-bis(3,5-di-*tert*-butyl-4-hydroxyphenyl)-[2,2'-bithiophene]-3,3'-dicarbaldehyde (ACO) (30 mg, 0.0475 mmol) in CH₂Cl₂ (10 mL), MnO₂ (30 mg) was added. The resulting mixture was stirred until the starting material was completely reacted (≈ 2 hours 30 minutes). The reaction mixture was filtered and the organic solvent was removed under reduced pressure. The desired product was collected as an iridescent dark green/red solid in quantitative yield.

¹H-NMR (400 MHz, CDCl₃): δ = 9.5–7.3 (br. m), 1.48 ppm (s; *t*-Bu). HRMS (ESI): *m/z* calcd for C₃₈H₄₄O₆S₂ + H⁺: 661 [M + H⁺], found: 661.7 (M⁺).

4-Bromo-2,6-dimethoxyphenol (20). 2,6-Dimethoxyphenol (1.0 g, 6.5 mmol) was dissolved in CHCl_3 (10 mL). EtOH (0.08 mL) and 50% NaH solution (3 mg, 0.13 mmol) were added and the mixture was cooled to -78°C . NBS (1.15 g, 6.48 mmol) was added portionwise and the mixture stirred at this temperature for 1 hour. Then the cooling bath was removed and the mixture stirred at room temperature for 30 min and at 65°C for 5 min. The reaction mixture was allowed to cool to room temperature and the solvent was removed under reduced pressure. The yellowish residue obtained was dissolved in diethyl ether and filtered. The solvent was evaporated to obtain a yellow solid which was stirred in heptane (12 mL) at 85°C for 15 min. The yellowish-brown oil was filtered through a celite pad. The filtrate was allowed to recrystallize to give 1.0 g of the desired product as a white solid (66% yield).

$^1\text{H-NMR}$ (400 MHz, CDCl_3): δ = 6.73 (s, 2H; Ph-H), 5.41 (s, 1H; -OH), 3.88 ppm (s, 6H; $-\text{OCH}_3$).

4,4'-([2,2'-Bithiophene]-5,5'-diyl)-bis(2,6-dimethoxyphenol) (AMeOMeO)

Method A. A solution of 4-bromo-2,6-dimethoxyphenol (**20**) (52 mg, 0.224 mmol), 5,5'-bis(trimethylstannyl)-2,2'-bithiophene (50 mg, 0.102 mmol), and $\text{Pd}(\text{PPh}_3)_4$ (12 mg, 0.01 mmol) in anhydrous toluene was thoroughly mixed in a process vial. The vial was capped and the mixture was heated under microwave irradiation conditions at 150°C and 150 W for 53 minutes, then the process vial was allowed to cool to room temperature. The reaction mixture was extracted with ethyl acetate and the organic fractions were combined, dried over Na_2SO_4 and filtered. After solvent removal, the raw product was purified using flash chromatography (silica gel, 7:3 hexane:ethyl acetate) to afford 15 mg (32% yield) of **AMeOMeO** as a yellow solid.

Method B. A solution of 4-bromo-2,6-dimethoxyphenol (325 mg, 1.40 mmol), $\text{Pd}(\text{PPh}_3)_4$ (70 mg, 0.061 mmol) and 5,5'-bis(trimethylstannyl)-2,2'-bithiophene (300 mg, 0.61 mmol) in anhydrous toluene (52 mL) was refluxed for 5 hours. Then it was allowed to cool to room temperature, poured into water and extracted with ethyl acetate. The organic fractions were combined together, dried over Na_2SO_4 , filtered, and then the solvent was removed under reduced pressure. The raw product was purified using flash chromatography (silica gel, 1:1 hexane:ethyl acetate) to afford 88 mg (30% yield) of **AMeOMeO** as a dark yellow solid.

Method C. A solution of 4-bromo-2,6-dimethoxyphenol (**20**) (50 mg, 0.215 mmol) and 5,5'-bis(4,4,5,5-tetramethyl-1,3,2-dioxaborolan-2-yl)-2,2'-bithiophene (41 mg, 0.09 mmol), Na_2CO_3 (86 mg, 0.81 mmol) aqueous solution (1 M) and $\text{Pd}(\text{PPh}_3)_4$ (10 mg, 0.009 mmol) in previously degassed DME (2:1 with respect to water) were thoroughly mixed in a process vial. The vial was capped and the mixture was heated under microwave irradiation conditions at 130°C and 150 W for 42 min, then the process vial was allowed to cool to room temperature. The reaction mixture was extracted with ethyl acetate and the organic fractions were combined, dried over Na_2SO_4 and filtered. After solvent removal, the raw product was purified using flash chromatography (silica gel, 7:3 hexane:ethyl acetate) to afford 3 mg (7% yield) of **AMeOMeO** as a yellow solid.

$^1\text{H-NMR}$ (400 MHz, CDCl_3): δ = 7.13 (d, $^3J(\text{H,H})$ = 3.71 Hz, 2H; thiophene), 7.12 (d, $^3J(\text{H,H})$ = 3.71 Hz, 2H; thiophene), 6.82 (s, 4H; phenyl-H), 5.55 (s, 2H; -OH), 3.96 ppm (s, 12H; $-\text{OCH}_3$); HRMS (ESI): m/z calcd for $\text{C}_{24}\text{H}_{22}\text{O}_6\text{S}_2 + \text{Na}^+$: 493 [$\text{M} + \text{Na}^+$], found: 493.4 ($\text{M} + \text{Na}^+$).

The monosubstituted product, 4-([2,2'-bithiophen]-5-yl)-2,6-dimethoxyphenol (**22**), was obtained as the main product in Method C (yield 46%), but as a by-product in Methods A and B: $^1\text{H-NMR}$ (400 MHz, CDCl_3): δ = 7.61 (br. d, 2H; Th-H), 7.39 (br. m, 2H; Th-H), 7.14 (br. m, 3H; Th-H), 6.83 (s, 2H; Ph-H), 5.55 (s, 1H; -OH), 3.96 ppm (s, 6H; $-\text{OCH}_3$).

5,5'-Bis(3,5-dimethoxy-4-oxo-2,5-cyclohexadien-1-ylidene)-5,5'-dihydro-2,2'-bithiophene (QMeOMeO). To a solution of **AMeOMeO** (5 mg, 0.012 mmol) in benzene (22 mL), $\text{K}_3\text{Fe}(\text{CN})_6$ (40 mg, 0.11 mmol) and a 0.1 M aqueous solution of KOH (67 mg, 1.1 mmol) were added. The resulting mixture was stirred until the starting material was completely reacted (≈ 45 minutes). The reaction mixture was filtered and the solid was washed with toluene. The desired product was collected as a dark blue solid in quantitative yield.

HRMS (ESI): m/z calcd for $\text{C}_{24}\text{H}_{20}\text{O}_6\text{S}_2 + \text{H}^+$: 469 [$\text{M} + \text{H}^+$], found: 469.4 (M^+).

4,4'-([2,2'-Bithiophene]-5,5'-diyl)-bis(2-(trifluoromethyl)phenol) (ACF₃CF₃). To a solution of 4-bromo-2-(trifluoromethyl)phenol (**23**) (338 mg, 1.403 mmol) in anhydrous toluene (50 mL), $\text{Pd}(\text{PPh}_3)_4$ (80 mg, 0.0609 mmol) and 5,5'-bis(trimethylstannyl)-2,2'-bithiophene (**24**) (300 mg, 0.6099 mmol) were rapidly mixed. The resulting mixture was refluxed for 14 hours. Then it was allowed to cool to room temperature, poured into water and extracted with ethyl acetate. The organic fractions were combined together, dried over Na_2SO_4 , filtered, and then the solvent was removed under reduced pressure. The raw product was purified using flash chromatography (silica gel, 1:1 hexane:dichloromethane) to afford 160 mg (54% yield) of **ACF₃CF₃** as a dark yellow solid.

$^1\text{H-NMR}$ (400 MHz, CDCl_3): δ = 7.72 (d, $^4J(\text{H,H})$ = 1.76 Hz, 2H; phenyl-H), 7.63 (dd, $^3J(\text{H,H})$ = 8.59 Hz, $^4J(\text{H,H})$ = 1.76 Hz, 1H; phenyl-H), 7.15 (s, 4H; thiophene), 7.00 (d, $^3J(\text{H,H})$ = 8.39 Hz, 1H; phenyl-H), 6.82 (s, 2H; phenyl-H), 5.55 (s, 1H; -OH), 5.52 (s, 1H; -OH), 3.96 ppm (s, 6H; $-\text{OCH}_3$);

HRMS (ESI): m/z calcd for $\text{C}_{22}\text{H}_{12}\text{F}_6\text{O}_2\text{S}_2 - \text{H}^+$: 485 [$\text{M} - \text{H}^+$], found: 485.3 ($\text{M} - \text{H}^+$).

5,5'-Bis(3-trifluoromethyl-4-oxo-2,5-cyclohexadien-1-ylidene)-5,5'-dihydro-2,2'-bithiophene (QCF₃CF₃). To a solution of **ACF₃CF₃** (4 mg, 0.0082 mmol) in benzene (4.1 mL), $\text{K}_3\text{Fe}(\text{CN})_6$ (27 mg, 0.082 mmol) and a 0.4 M aqueous solution of KOH (46 mg, 0.82 mmol) were added. The resulting mixture was stirred until the starting material was completely reacted (≈ 1 hour). The reaction mixture was filtered and the solid was washed with toluene. The desired product was collected as a dark green solid in quantitative yield.

HRMS (ESI): m/z calcd for $\text{C}_{22}\text{H}_{10}\text{F}_6\text{O}_2\text{S}_2 + \text{H}^+$: 485 [$\text{M} + \text{H}^+$], found: 485.3 (M^+).

4-(5'-(4-Hydroxy-3-(trifluoromethyl)phenyl)-[2,2'-bithiophen]-5-yl)-2,6-dimethoxyphenol (AMeOCF₃). A solution of 4-bromo-2-(trifluoromethyl)phenol (**23**) (252 mg, 1.05 mmol), 4-bromo-2,6-dimethoxyphenol (**20**) (244 mg, 1.05 mmol), $\text{Pd}(\text{PPh}_3)_4$ (97 mg,

0.105 mmol) and 5,5'-bis(trimethylstannyl)-2,2'-bithiophene (24) (415 mg, 0.844 mmol) in anhydrous toluene (60 mL) was refluxed for 5 hours. Then it was allowed to cool to room temperature, poured into water and extracted with ethyl acetate. The organic fractions were combined together, dried over Na_2SO_4 , filtered, and then the solvent was removed under reduced pressure. The raw product was purified using flash chromatography (silica gel, 1 : 1 hexane : ethyl acetate) to afford 140 mg (34% yield) of AMeOCF_3 as a dark yellow solid. 4,4'-[[2,2'-bithiophene]-5,5'-diyl]-bis(2-(trifluoromethyl)phenol) (ACF_3CF_3) and 4,4'-[[2,2'-bithiophene]-5,5'-diyl]-bis(2,6-dimethoxyphenol) (AMeOMeO) were obtained as by-products, respectively, in 9.5% (39 mg) and 4% (16 mg) yields.

$^1\text{H-NMR}$ (400 MHz, CDCl_3): δ = 7.72 (d, $^4J(\text{H,H})$ = 1.37 Hz, 1H; Ph-H), 7.64 (dd, $^3J(\text{H,H})$ = 8.59 Hz, $^4J(\text{H,H})$ = 1.95 Hz, 1H; Ph-H), 7.14 (m, 4H; Th-H), 7.00 (d, $^3J(\text{H,H})$ = 8.59 Hz, 1H; Ph-H), 6.82 (s, 2H; Ph-H), 5.55 (s, 1H; -OH), 5.52 (s, 1H; -OH), 3.96 ppm (s, 6H; -OCH₃); HRMS (ESI): m/z calcd for $\text{C}_{23}\text{H}_{17}\text{F}_3\text{O}_4\text{S}_2 - \text{H}^+$: 477 [$\text{M} - \text{H}^+$], found: 477.4 ($\text{M} - \text{H}^+$).

2,6-Dimethoxy-4-(5'-(4-oxo-3-(trifluoromethyl)cyclohexa-2,5-dien-1-ylidene)-[2,2'-bithiophenylidene]-5-ylidene)cyclohexa-2,5-dienone (QMeOCF_3). To a solution of AMeOCF_3 (5 mg, 0.0105 mmol) in benzene (21 mL), $\text{K}_3\text{Fe}(\text{CN})_6$ (35 mg, 0.105 mmol) and a 0.1 M aqueous solution of KOH (59 mg, 1.05 mmol) were added. The resulting mixture was stirred until the starting material was completely reacted (\approx 1 hour 30 minutes). The reaction mixture was filtered and the solid was washed with toluene. The desired product was collected as a dark green solid in quantitative yield.

HRMS (ESI): m/z calcd for $\text{C}_{23}\text{H}_{15}\text{F}_3\text{O}_4\text{S}_2 + \text{H}^+$: 477 [$\text{M} + \text{H}^+$], found: 477.3 (M^+).

Measurements and characterization

$^1\text{H-NMR}$ spectra were collected using a Bruker ARX 400 NMR spectrometer. Mass spectrometry was carried out with a Bruker Esquire 3000 Plus mass spectrometer. UV-vis absorption spectra were recorded with a Cary 5000 spectrophotometer (Varian). Raman spectra were recorded with a Nicolet FT-Raman Nexus NXR 9650 that employs a Nd/YAG laser with excitation at λ = 1064 nm and a Horiba Jobin Yvon LabRam HR800 with excitation light at 632 nm. The X-ray data were collected on a Bruker X8 Prospector APEX-II/CCD diffractometer using Cu K α radiation (λ = 1.54050 Å). The structure was solved by direct methods and refined using the SHELX-97 package.²³

X-ray crystallographic analysis

CCDC-1029034.

Acknowledgements

This work was partly supported by Fondazione Cariplo through the project INDIXI (Grant no. ref. 2011/0368). E.P. thanks the European Union for financial support ("Marie Curie" FP7 IRG grant no. 268231).

Notes and references

- 1 J. C. Ribierre, S. Watanabe, M. Matsumoto, T. Muto, D. Hashizume and T. Aoyama, Thickness Dependence of the Ambipolar Charge Transport Properties in Organic Field-Effect Transistors based on a Quinoidal Oligothiophene Derivative, *J. Phys. Chem. C*, 2011, **115**(42), 20703–20709.
- 2 T. Agostinelli, M. Caironi, D. Natali, M. Sampietro, G. Dassa, E. V. Canesi, C. Bertarelli, G. Zerbi, J. Cabanillas-Gonzalez, S. De Silvestri and G. Lanzani, A planar organic near infrared light detector based on bulk heterojunction of a heteroquarterphenoquinone and poly[2-methoxy-5-(2[^{sup}]-ethyl-hexyloxy)-1,4-phenylene vinylene], *J. Appl. Phys.*, 2008, **104**(11), 114508.
- 3 Z. Kan, L. Colella, E. V. Canesi, G. Lerario, R. S. S. Kumar, V. Bonometti, P. R. Mussini, G. Cavallo, G. Terraneo, P. Pattanasattayavong, T. D. Anthopoulos, C. Bertarelli and P. E. Keivanidis, Triple bulk heterojunctions as means for recovering the microstructure of photoactive layers in organic solar cell devices, *Sol. Energy Mater. Sol. Cells*, 2014, **120**, 37–47.
- 4 J. Thiele, Create PDF files without this message by purchasing novaPDF printer (<http://www.novapdf.com>), *Chem. Ber.*, 1904, **37**, 1463.
- 5 A. E. Chichibabin, A. E. Chichibabin, *Chem. Ber.*, 1907, **40**, 1810.
- 6 L. K. Montgomery, J. C. Huffman, E. A. Jurczak and M. P. Grendze, The Molecular Structures of Thiele's and Chichibabin's Hydrocarbons, *J. Am. Chem. Soc.*, 1986, **108**, 6004–6011.
- 7 R. Ponce Ortiz, J. Casado, S. Rodríguez González, V. Hernández, J. T. López Navarrete, P. M. Viruela, E. Ortí, K. Takimiya and T. Otsubo, Quinoidal oligothiophenes: towards biradical ground-state species, *Chem. – Eur. J.*, 2010, **16**(2), 470–484.
- 8 K. Takahashi and T. Suzuki, p-Diphenoquinone Analogues Extended by Dihydrothiophenediylidene Insertion: A Novel Amphoteric Multistage Redox System, *J. Am. Chem. Soc.*, 1989, **111**(14), 5483–5485.
- 9 K. Takahashi and S. Tarutani, Efficient Synthesis of 2-Iodo and 2-Dicyanomethyl Derivatives of Thiophene, Selenophene, Tellurophene, and Thieno[3,2-b]thiophene, *Heterocycles*, 1996, **43**(9), 1927–1935.
- 10 M. Kozaki, A. Isoyama and K. Okada, Detection of a diradical intermediate in the *cis-trans* isomerization of 5,5'-bis(4,5-diphenyl-2H-imidazol-2-ylidene)-5,5'-dihydro-bithiophene, *Tetrahedron Lett.*, 2006, **47**(30), 5375–5378.
- 11 M. Kozaki, A. Isoyama, K. Akita and K. Okada, Preparation, properties, and reduction of heteroaromatic quinoids with 1,4-diazacyclopentadien-2-ylidene terminals, *Org. Lett.*, 2005, **7**, 115–118.
- 12 D. Fazzi, E. V. Canesi, F. Negri, C. Bertarelli and C. Castiglioni, Biradicaloid character of thiophene-based heterophenoquinones: the role of electron-phonon coupling, *ChemPhysChem*, 2010, **11**(17), 3685–3695.
- 13 E. V. Canesi, D. Fazzi, L. Colella, C. Bertarelli and C. Castiglioni, Tuning the quinoid *versus* biradicaloid character of thiophene-based heteroquarterphenoquinones by

- means of functional groups, *J. Am. Chem. Soc.*, 2012, **134**(46), 19070–19083.
- 14 G. Zotti, M. C. Gallazzi, G. Zerbi and S. V. Meille, Conducting polymers from anodic coupling of some regiochemically defined dialkoxy-substituted thiophene oligomers, *Synth. Met.*, 1995, **73**(3), 217–225.
 - 15 M. C. Gallazzi, F. Toscano, D. Paganuzzi, C. Bertarelli, A. Farina and G. Zotti, Polythiophenes with Unusual Electrical and Optical Properties Based on Donor Acceptor Alternance Strategy, *Macromol. Chem. Phys.*, 2001, **202**(10), 2074–2085.
 - 16 S. Di Motta, F. Negri, D. Fazzi, C. Castiglioni and E. V. Canesi, Biradicaloid and Polyenic Character of Quinoidal Oligothiophenes Revealed by the Presence of a Low-Lying Double-Exciton State, *J. Phys. Chem. Lett.*, 2010, **1**(23), 3334–3339.
 - 17 M. B. S. J. March, *March's Advanced Organic Chemistry*, 2012.
 - 18 Y. Suzuki, E. Miyazaki and K. Takimiya, ((Alkyloxy)carbonyl)-cyanomethylene-Substituted Thienoquinoidal Compounds: a New Class of Soluble n-Channel Organic Semiconductors for Air-Stable Organic Field-Effect Transistors, *J. Am. Chem. Soc.*, 2010, **132**(30), 10453–10466.
 - 19 M.-H. Yoon, A. Facchetti, C. E. Stern and T. J. Marks, Fluorocarbon-modified organic semiconductors: molecular architecture, electronic, and crystal structure tuning of arene- versus fluoroarene-thiophene oligomer thin-film properties, *J. Am. Chem. Soc.*, 2006, **128**(17), 5792–5801.
 - 20 S. A. Lee, S. Hotta and F. Nakanishi, Spectroscopic Characteristics and Intermolecular Interactions of Thiophene/Phenylene Co-Oligomers in Solutions, *J. Phys. Chem. A*, 2000, **104**(9), 1827–1833.
 - 21 C. Castiglioni, M. Tommasini and G. Zerbi, Raman spectroscopy of polyconjugated molecules and materials: confinement effect in one and two dimensions, *Philos. Trans. R. Soc. London, Ser. A*, 2004, **362**, 2425–2459.
 - 22 K. Takahashi, T. Suzuki, K. Akiyama and Y. Fukazawat, Synthesis and Characterization of Novel p-Terphenyl-quinone Analogues Involving a Central Dihydrothiophenediylidene Structure, *J. Am. Chem. Soc.*, 1991, **113**(12), 4576–4583.
 - 23 G. M. Sheldrick, A short history of SHELX, *Acta Crystallogr., Sect. A: Found. Crystallogr.*, 2008, **64**, 112–122.